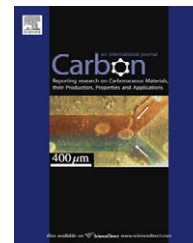


available at www.sciencedirect.comjournal homepage: www.elsevier.com/locate/carbon

The release of free standing vertically-aligned carbon nanotube arrays from a substrate using CO₂ oxidation

Jia-Qi Huang, Qiang Zhang¹, Meng-Qiang Zhao, Fei Wei*

Beijing Key Laboratory of Green Chemical Reaction Engineering and Technology, Department of Chemical Engineering, Tsinghua University, Beijing 100084, China

ARTICLE INFO

Article history:

Received 19 November 2009

Accepted 16 December 2009

Available online 23 December 2009

ABSTRACT

Free standing vertically-aligned carbon nanotube (CNT) arrays were released from a quartz substrate on a large scale by using CO₂ as an oxidative reagent to weaken the array-substrate interaction and facilitate their harvest. During the oxidation process, amorphous carbon and carbon in contact with metallic particles were preferentially etched, leading to the easy release of high quality free standing CNT arrays. O₂ was also used as an oxidant for comparison. The O₂ showed a stronger oxidizability and caused the formation of CNTs with a turbostratic-graphitic carbon heterojunction structure. The mechanisms of CO₂ and O₂ oxidation of CNT arrays were investigated, and based on these results, CO₂ was considered a more suitable oxidant for the purpose.

© 2009 Elsevier Ltd. All rights reserved.

1. Introduction

Free standing vertically-aligned carbon nanotube (VACNT) arrays have been one of the focuses in nanoscience profiting from their unique properties such as: approximately parallel arrangement, high purity and similar length for individual carbon nanotube (CNT). To this day, free standing CNT arrays can be served directly as electrodes, super spring, membrane, field emission display, battery and supercapacitor. They can be sheared into fluffy CNTs and further dispersed into super long individual CNTs for transparent conductive film, bucky-paper, etc. Significant improvements in the electronic, mechanical, and thermal properties of polymers after CNT reinforcement were demonstrated as well. Those applications will be realized if free standing CNT arrays can be produced at a large scale.

CNT arrays have to be grown on certain substrates (such as silica templates, silicon wafers, quartz plates, ceramic spheres, lamellar clay, carbon fibers, etc.) through chemical vapor deposition (CVD). The as-grown CNT arrays are commonly attached to the surface of substrates. Various methods

have been proposed to release free standing CNT arrays from the substrates. The most common method is dissolving the substrates (such as anodic aluminum oxide removing by base solution [1], silicon wafer and quartz can be removed by emerging in hydrofluoric acid (HF) solution [2]). Simple mechanical pressing method was also used by Zhu et al. to transport the VACNT arrays from the silicon wafer to metallic surface [3]. Other mechanical methods such as mechanical traction and separation by peeling with blades were also carried out to release the arrays from the substrates [4,5]. Sometimes, sonicating the as-grown products in water is also effective for the release of CNT array from spherical substrates [6]. Recently, Murakami and Maruyama found that water can serve as the medium for the separation of CNT arrays by conquering the array-substrate interaction with surface tension, which was more efficient but additional contaminations may be introduced in the process [7]. Up to now, the methods that were mentioned above were not effective enough to meet the requirements of a large-scaled harvest of free standing CNT arrays from various substrates. Furthermore, due to the strong interactions between CNT arrays and

* Corresponding author: Fax: +86 10 62772051.

E-mail address: wf-dce@tsinghua.edu.cn (F. Wei).

¹ Present address: Department of Chemical Engineering, Case Western Reserve University, Cleveland, OH 44106, USA. 0008-6223/\$ - see front matter © 2009 Elsevier Ltd. All rights reserved.

doi:10.1016/j.carbon.2009.12.038

the substrates, the original structures of the CNT arrays are commonly destroyed during the traditional separation procedures. A highly effective engineering method for the release of free standing CNT array from different substrates should be developed.

The key to release free standing CNT array is to break the strong connection between the substrate and the as-grown CNT arrays. The interaction between CNTs and substrate was the driving force for the self-organization of CNTs into array structure [8]. But the strong interaction remained to be an obstacle for further application of CNT arrays, which needs to be weakened after the growth of CNT arrays. Recently, it was reported that the addition of oxidative reagents (such as H₂O, CO₂ and O₂) during the growth process can improve the activity and prolong the lifetime of catalyst, and thus enhanced the growth of VACNT arrays [3,5,9–15]. Water steam was also used to promote the release of single-walled CNT arrays by etching the precipitated carbon between the catalyst and the CNTs [15]. Some applications after the release were also developed, including the observation of electron hopping, fabrication of terahertz polarizer, etc [16–18]. However, the detailed understanding of whole oxidation process needs to be provided in order to guide the large-scale application of this process. Here, we select CO₂ instead of water steam as the oxidant mainly due to the convenience in the industrial applications and the proper oxidizability. The introduction of CO₂ after the growth of CNT arrays can significantly weaken the array–substrate interactions and selectively etch the amorphous carbon decorated on CNTs. Compared with water steam and O₂, CO₂ were considered as a more suitable oxidant in the release of CNT arrays. An engineering approach for the release of free standing CNT array was proposed.

2. Experimental

The CNT arrays were synthesized on quartz plates (size: 30 × 10 × 2.0 mm) and the inner surface of the quartz tube through floating catalyst method [6,19,20] by means of using ferrocene as the catalyst precursor and xylene as the carbon source. The concentration of the ferrocene in xylene was 10 g/l. The quartz plates were used as the growth substrates and were placed in the center of a horizontal quartz tube (inner diameter of 30 mm and length of 1500 mm), which was set in a tubular furnace. The xylene solution was injected into the reactor with a feed rate of 6.0 ml/h using a motorized syringe pump after the react temperature reached 800 °C under carrier gas, which was composed of 600 sccm Ar and 40 sccm H₂. After the growth of CNT array, the feed of xylene solution and hydrogen were terminated. Then, the temperature of the reaction zone was left to be cooled down to 700 °C and the oxidative reagent (carbon dioxide or oxygen) was introduced into the reactor. The oxidation atmosphere lasted for half an hour under 700 °C, and then the furnace cooled down to room temperature under Ar protection. For a typical experiment, the concentration of CO₂ and O₂ was 4000 and 100 ppm, respectively for oxidation.

After the whole process, the product was lightly pushed out from the quartz tube for further characterization. Photos of the as-grown products were taken using a Ricoh R4 video

camera. High-resolution scanning electron microscopy (SEM, JSM 7401F, at 5.0 kV) was used to characterize the morphology of the CNT arrays. High-resolution transmission electron microscopy (TEM, JEM 2010, at 120.0 kV) was used to observe the detailed structure of CNTs in the arrays. Raman spectroscopy of the CNTs was performed using a Raman microscope (Renishaw, RM2000, He–Ne laser excitation line 633.0 nm). The thermal gravimetric analysis (TGA) under CO₂ atmosphere was also carried out to test the content of amorphous and graphite carbon in the sample with a temperature ramp rate of 10 °C/min and a CO₂ feed rate of 30 ml/min.

3. Results and discussion

3.1. The release of free standing CNT arrays by CO₂ oxidation

Following common CVD procedure for synthesis of CNT array, the derived array was firmly attached to the quartz substrate [4]. When the array was peeled off, the obtained CNT film will crack into small blocks during mechanical separation process due to the strong array–substrate interaction [21]. For comparison, post CO₂ oxidation was employed to facilitate the release of VACNT array from the substrate. Fig. 1a and b showed the free standing CNT arrays separated from the inner surface of the quartz tube and quartz plate, respectively. After the oxidation treatment, the adhesive force between the CNT array and the substrate was significantly reduced. Therefore, the free standing CNT arrays can be easily obtained by a light push. The original shape of the as-grown array can be well preserved. VACNT arrays with a tubular structure can be obtained due to the weak CNTs–substrate interaction (Fig. 1a). Furthermore, it can be seen from Fig. 1b that after the detachment of arrays from the quartz plate, nearly no CNTs remained on the quartz substrate. After the separation of CNT arrays, the quartz plate can be served as the substrate for the growth of CNT arrays again. Benefiting from the weak array–substrate interaction, some engineering mechanical treatments, such as mechanical vibration and gas flow shearing can also be used to release VACNT arrays from different substrates at a large scale.

3.2. Comparison of free standing CNT arrays obtained with/without CO₂ oxidation

To show the advantage of the release process for free standing CNT arrays by CO₂ oxidation, the morphologies and structures of CNTs were carefully analyzed by SEM, TEM, TGA, and Raman spectra. The VACNT arrays obtained without CO₂ oxidation were peeled off by using blades and characterized for comparison. Fig. 2a showed the top surface morphology of the VACNT arrays obtained without CO₂ oxidation. Due to the deposition of exceeded metallic catalyst particles and the accumulation of pyrolysis carbonaceous impurities during floating catalyst CVD, the top of the free standing VACNT arrays were coated with impurities and numerous catalyst particles [8]. In contrast, a lot of large Fe₂O₃ particles with the size of about 200 nm were found on the top surface of the CNT arrays obtained with CO₂ oxidation (Fig. 2b). On the

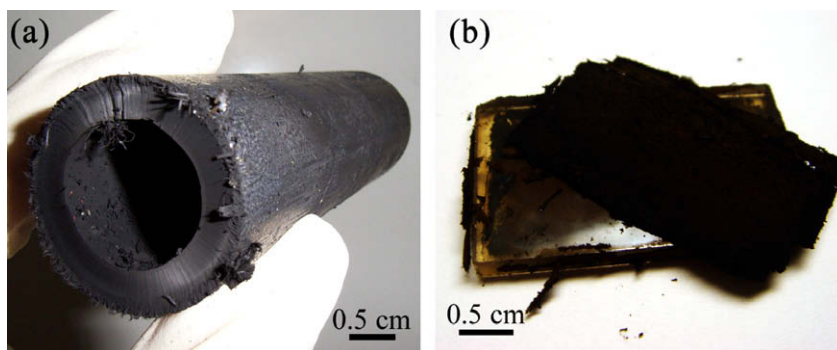


Fig. 1 – Free standing block of CNT arrays separated from (a) the inner surface of quartz tube and (b) the quartz plate.

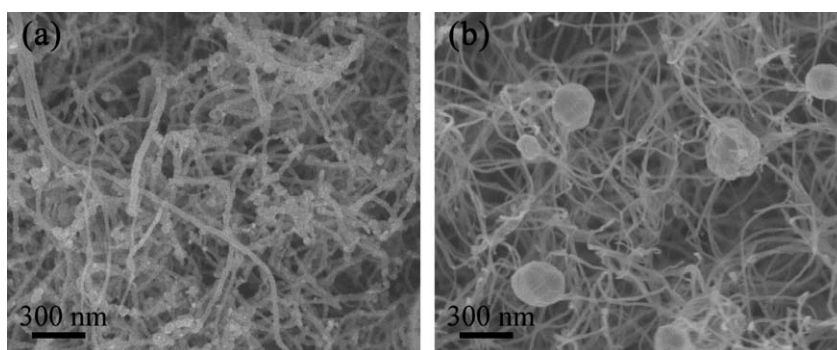


Fig. 2 – The top surface of the CNT array (a) without CO₂ oxidation and (b) with CO₂ oxidation.

other hand, when compared with the original VACNT arrays, the diameter of CNTs was significantly decreased, and the side wall of the CNTs in array became much cleaner. CO₂ served as oxidative reagent at 700 °C and reacted with the as-deposited carbon materials. Compared with well-crystallized graphite layers, amorphous carbon, turbostratic carbon and carbon in contact with metallic catalyst particles were relatively unstable, and they were thus preferentially etched [19,22,23]. Metal-encapsulated carbon spheres were easily oxidized and left bare metal particles. Due to the high surface energy of metal, the particles were prone to sinter into large catalyst particles with a size of 100–250 nm (Fig. 2b).

Furthermore, the bottom of the derived free standing CNT arrays also possessed different morphologies. As is shown in Fig. 3a, the roots of CNTs in the arrays by means of blade peeling exhibited clear orientation, which was caused by the strong array-substrate interaction and the damage of blades. The CNTs on the root ruptured due to the shear strength during the blade peeling process and few catalyst particles can be found at the root of CNTs (Fig. 3b). The arrays obtained by floating catalyst process commonly consisted of CNTs covering a wide range of diameters. Numerous thin CNTs can be observed in Fig. 3b as well as the thick ones. The diameter distributions of the CNTs in the array were obtained by the statistics based on the side view of the CNT arrays. The diameters of CNTs ranged from 20 to 70 nm, with a mean diameter of approximately 38 nm, showing good alignment (Fig. S1a and b). While for quartz substrate, there were catalyst particles with a density of approximately $1.7 \times 10^{14}/\text{m}^2$. Some ruptured CNT fragment can be found (indicated by

the arrows in Fig. 3c). Fig. 3d shows the fine structure of intrinsic CNTs without CO₂ treatment. The CNT was composed of over 50 graphic walls. Some decorated amorphous carbon can also be found, clinging on the exterior layer of CNT.

The free standing CNT arrays obtained by CO₂ oxidation showed flat bottom morphology, as illustrated in Fig. 4a. The CNTs maintained the intrinsic structure in the growth process. No evidence of damage can be observed due to the avoidance of strong mechanical force in the release process. Different from the mechanically fractured CNT roots, the morphologies of CNT roots were well preserved. Some CNTs were with catalyst particles, while others were free of catalyst particles (Fig. 4b). Fig. 4c showed the surface morphology of quartz substrate after the CNT array harvest based on CO₂ treatment. The density of catalyst particle left on the substrates decreased to $8 \times 10^{13}/\text{m}^2$ due to the sintering of catalyst particles. The size distributions of catalyst particles were also changed. The diameters of the remaining catalyst particles ranged from 30 to 110 nm, exhibiting an average diameter of 58 nm (Fig. 4c). While the catalyst particles remained on quartz plate without CO₂ oxidative treatment, and they were with an average diameter of 39 nm, distributing from 20 to 60 nm (Fig. 3c). Furthermore, some concave structures can be found on the surface of quartz plate after CO₂ oxidation (Fig. 4c), the size of which ranged from several tens to one hundred nanometers. These concave structures were speculated to correspond to the large-sized catalyst particles attached to the roots of some CNTs. Moreover, the side views of free standing VACNT arrays showed good alignment

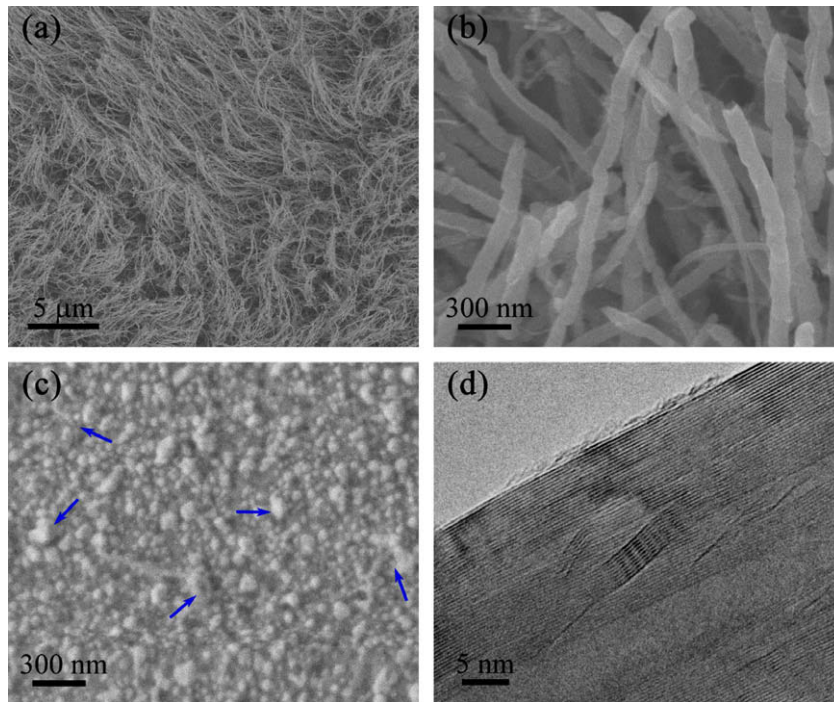


Fig. 3 – (a) Low magnification and (b) high magnification SEM image of the bottom of free standing CNT arrays without CO₂ oxidation; (c) the morphology of quartz substrate after removing the VACNT arrays without CO₂ oxidation; (d) the high resolution TEM image of CNT without CO₂ oxidation.

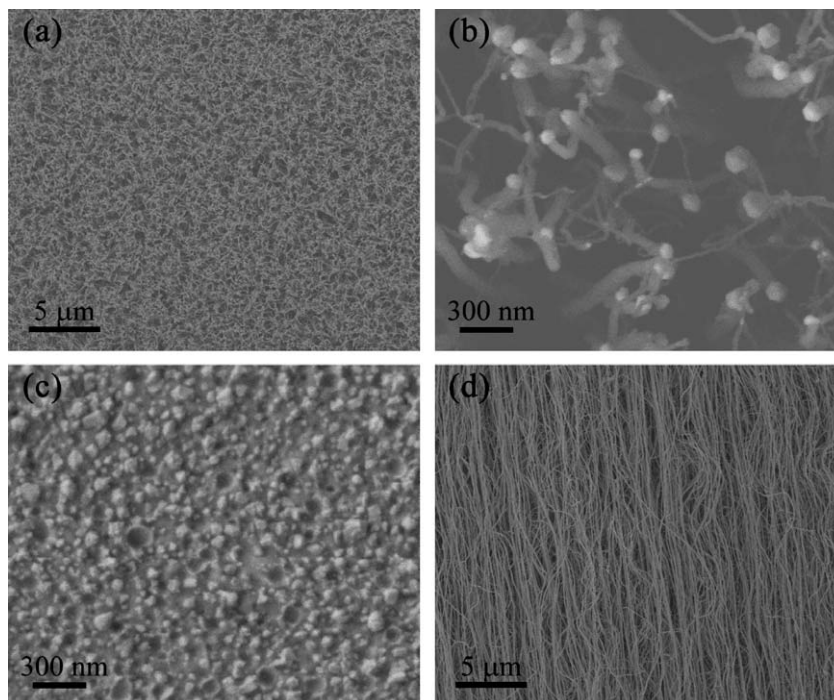


Fig. 4 – (a) Low magnification and (b) high magnification SEM image of the bottom of free standing CNT arrays with CO₂ oxidation; (c) the morphology of quartz substrate after the release of VACNT arrays using CO₂ oxidation; (d) the side view of free standing VACNT arrays with CO₂ oxidation.

(Fig. 4d), which indicates the array structure was preserved during the whole process based on CO₂ oxidation. It was also noticed that the diameter of CNTs were about 15–40 nm at the

top of the array, with an average diameter of 27 nm (Fig. S1c). Near the roots of the CNT arrays, the diameters of CNTs ranged from 20 to 70 nm, which obviously did not change during

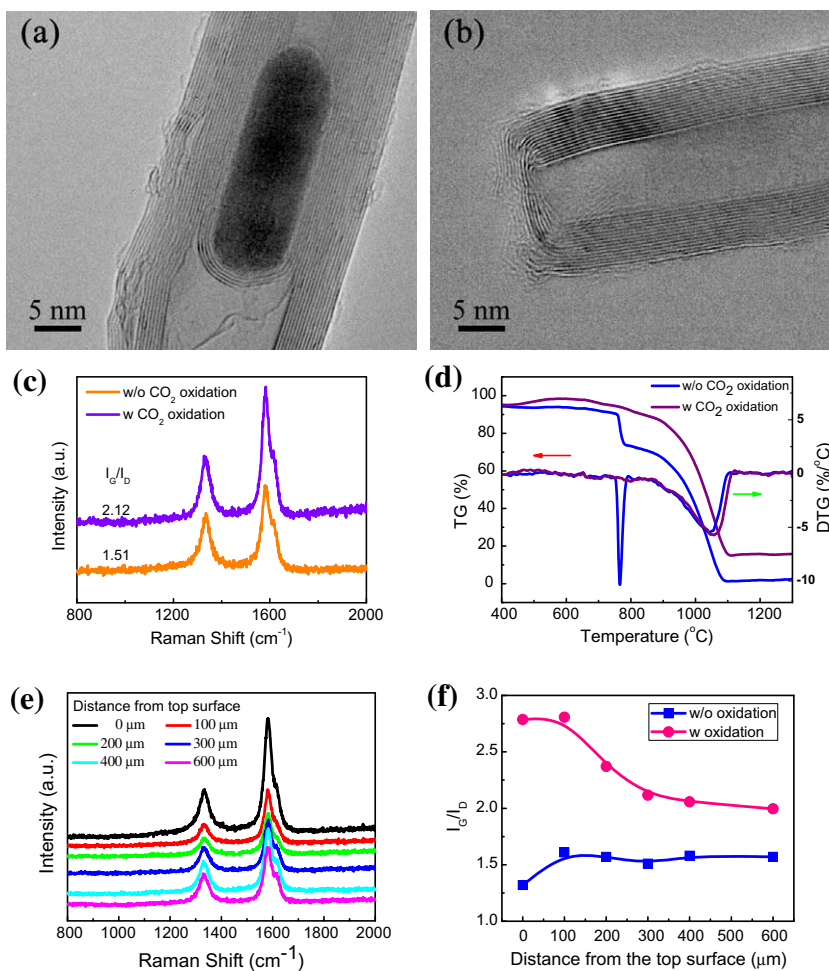


Fig. 5 – (a and b) The high resolution TEM images of CNTs with CO₂ oxidation; (c) the Raman spectra and (d) TGA curve of free standing CNT arrays with CO₂ oxidation; (e) Raman spectra on the side of the CNT arrays with CO₂ oxidation (0, 100, 200, 300, 400 and 600 μm from the top); (f) the I_G/I_D values at different positions on the side wall of pristine and oxidized CNT arrays.

the CO₂ oxidation (Fig. S1d). The details will be discussed later.

TEM images were also obtained in order to characterize the fine structure of as obtained CNTs. Besides the desirable feature of easy release of VACNT arrays, the introduction of CO₂ can also improve the quality of VACNT arrays. During the CO₂ oxidation process, the amorphous carbon was relatively unstable and was preferentially etched [9–13,24]. However, the CO₂ oxidation removed the graphite walls of CNTs inevitably, which caused a decrease of the mean CNT diameter from 38 to 32 nm. Fig. 5a showed the HRTEM image of one few-walled CNT with a wall number of 14, in which the graphite layer was clean and there were only a few defects found in the walls of the CNT. The end of CNT, shown in Fig. 5b, has a curvature structure and contained non-hexagon carbon rings, which resulted in the instability in the oxidative atmosphere compared with the side wall. Some graphite layers at the end of the CNT were damaged while the end had not been completely opened. The Raman spectra in Fig. 5c were employed to illustrate the crystallization degree of CNTs. The values of I_G/I_D (intensity ratio of G band to D band) were 2.12 for CNT arrays with the CO₂ treatment, which was much higher than that without CO₂ treatment (1.51), revealing the improvement

in crystallization and lower content of impurities (Fig. 5c). This result consisted well with the TGA results under CO₂ atmosphere (Fig. 5d), in which the weight loss peak corresponded to the amorphous carbon (near 770 °C in Fig. 5d) disappeared for the samples with CO₂ oxidation, indicating the elimination of the amorphous carbon and higher purity of the CNT arrays using CO₂ oxidation.

The height of CNT arrays synthesized in floating catalyst process can be as tall as about 1.0 mm, in which the CNTs were densely packed. When the oxidation process occurred, the concentration of oxidant differed a lot at the top and the bottom of the CNT arrays with the view of diffusion resistance and reaction consumption. Raman spectra were employed to illustrate the difference in the degree of oxidation induced by the concentration gradient. The Raman spectra and the values of I_G/I_D in different positions (0, 100, 200, 300, 400 and 600 μm from the top of arrays) of CNT arrays after CO₂ oxidation were shown in Fig. 5e and f. As can be seen from Fig. 5f, the value of I_G/I_D was as high as 2.78 at the top of CNT array, indicating a relatively high crystallization degree of the graphite layers in the side walls of CNTs. With the distance away from the top increased, the value of I_G/I_D decreased gradually. At the point of 600 μm from the top,

the value of I_G/I_D was only 1.99, which is much lower than the top of CNT array. For comparison, the Raman results of the pristine CNT arrays without CO_2 oxidation were also presented (Raman spectra in Fig. S2 and curve of I_G/I_D value in Fig. 5f). The pristine CNT arrays shows relative low crystallization degree in the top of the array (I_G/I_D value of 1.31) and maintained a stable level in the rest parts (I_G/I_D value of around 1.55), which may resulted from the capture of more pyrolyzed carbon in the top part of arrays. Thus, the relatively higher crystallization degree should be attributed to the reaction feature of CO_2 as well as the concentration gradient in the CNT array. Under this specific condition, CO_2 reacted selectively with impurities, while the well-graphitized side walls of CNTs were preserved. Besides, the concentration of CO_2 decreased from the top to the bottom of CNT array. The relatively high concentration of CO_2 at the top of CNT array promoted the elimination of impurities and resulted in the highest value of I_G/I_D as indicated in Fig. 5f. It is also worth mentioning that all the points in the arrays were of higher I_G/I_D value than pristine CNT arrays, even at the bottom of arrays where the CO_2 concentration was the lowest. Actually, the gradient of CO_2 also led to the different CNT diameters in the whole CNT array. As indicated in Fig. S1, compared with the CNTs array without the oxidation, the diameter of CNTs near the top of CNT array obviously decreased to 15–40 nm while the diameter of CNTs at the bottom part (20–70 nm) hardly changed.

3.3. Synthesis of free standing graphitic–turbostratic CNT arrays by O_2 oxidation

The use of CO_2 improves the quality of CNT arrays and facilitates the release process due to the nature of oxidation. In addition to CO_2 , some other gaseous substance can serve as the oxidant in this process such as O_2 . Here, O_2 was used for the oxidative treatment instead of CO_2 for comparison. It was very interesting to find that the oxidation process was quite different in the case of O_2 oxidation. Fig. 6a shows the high resolution TEM image of the side wall of one CNT after the oxidation, which lasted 30 min under 500 ppm O_2 . It can be found that the exterior 10 walls of the CNT were composed of graphite layer segments, which were noticeably different from the interior walls. One metallic catalyst decorated on the side wall was also covered with turbostratic carbon segments. Core–shell-structured CNTs with radial turbostratic-graphite carbon heterojunction was fabricated in the free standing CNT array using O_2 oxidation. Similar graphitic–turbostratic CNT can be found in the CNTs oxidized under the O_2 concentration of 100 ppm as well (Fig. 6b). The generation of the turbostratic carbon can be ascribed to the stronger oxidizability of O_2 than that of CO_2 under the same temperature, leading to the faster oxidation with worse selectivity. Though array–substrate detachment and the elimination of the impurities can also be achieved by O_2 , the strong oxidizability of O_2 severely damaged the side walls of CNT and caused the generation of turbostratic carbon.

Raman characterization also indicated the different phenomena compared with CO_2 oxidation process (Fig. 6c and d). In the Raman spectra of free standing CNT arrays after O_2 oxidation under the O_2 concentration of 100 ppm (Fig. 6c),

the value of I_G/I_D were 1.39 and 1.69 for the top and bottom of the CNT array, respectively, indicating lower crystallization degree on the top than that on the bottom of CNT arrays. When under high O_2 concentration (the situation for the top of the array), though the impurities could be eliminated, the well-graphitized layers were oxidized into turbostratic carbon as well. In contrast, the O_2 concentration was relatively low at the bottom of CNT array, where the impurities could be oxidized similarly and the destruction of fine graphite layers was limited (Fig. 6d). The crystallization degrees of CNTs on the bottom were always higher when compared to the top array under various O_2 concentrations. Although the I_G/I_D value was higher than that of pristine CNT arrays due to the elimination of impurities, it was much lower than that of CO_2 -treated CNT arrays. Besides, the destruction on the side walls of CNTs in the O_2 oxidation process was serious, which reduced the quality of CNT arrays, indicating that CO_2 was a more suitable oxidant in this specific condition. Water steam was also used as the oxidizer for the release of CNT arrays. It shows similar ability to release the CNT arrays from the substrate while obtained CNT arrays exhibited some different characteristics (see Supplementary information).

3.4. Mechanism of free standing CNT array released by CO_2/O_2 oxidation

The high temperature reaction of carbon in an atmosphere of O_2 , H_2O and CO_2 has been widely studied by many groups and manufacturers to produce activated carbon [25–32] or CNTs [3,5,9–15,24]. The most significant advances in understanding the mechanism of reaction between molecular oxygen and carbon was carried out by the Walker Jr's research group [25,28]. Later, Radovic et al. [26,27] and Rodriguez-Reinoso et al. [30,31] also carried out a family of pioneer researches on the mechanisms of thermal activation by O_2 , CO_2 and water steam. They found that the entire process of activation depended on the selective gasification within a carbon particle, which was the consequence of a spectrum of reactivity within the carbon structures [32]. Recently, those oxidants were found to be great enhancers for the growth of CNTs [3,5,9–13,33,34]. For example, in the super growth of single-walled CNT array, the amount of introduced stream should be delicately controlled to prolong the life time of catalyst particles, and prevent the sintering of iron particles [5,34]. The effect of oxygen-containing gases have been investigated in the CVD for CNT growth, and they showed great ability to modulate the structure of CNTs [35]. In specific conditions, the stream can assist the opening of CNT end. Here, CO_2 and O_2 were used as enhancers to weaken the array–substrate interaction and modulate the structure of CNTs.

When CO_2 was introduced into the react chamber, it reacted with solid carbon through reproporation and generated CO as follows [32]:



in which a surface oxygen complex ($\text{C}(\text{O})$) was initially formed and subsequently became stable under the reaction conditions, acting as a retardant by blocking the reaction sites:



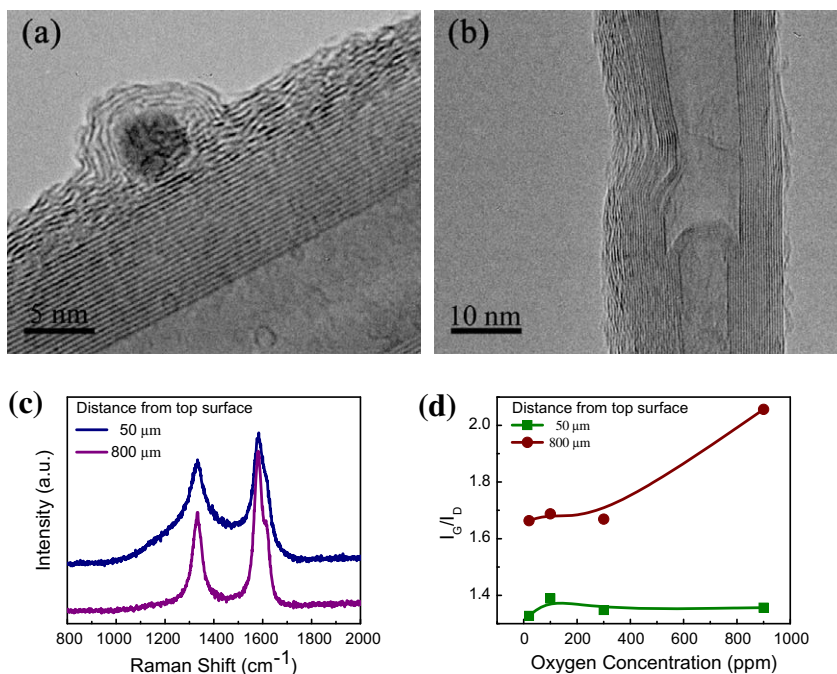


Fig. 6 – The high resolution TEM images of CNTs with O₂ oxidation under a O₂ concentration of (a) 500 ppm and (b) 100 ppm; (c) the Raman spectra of CNT array oxidized with 100 ppm O₂; (d) I_G/I_D value of free standing CNT arrays oxidized with different O₂ concentration.

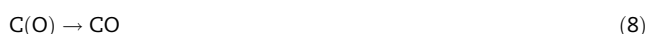
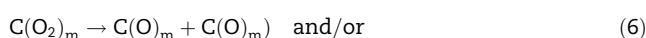
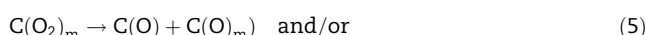
It may also decompose and leave the surface as CO



This process will leave a free surface carbon atom. The temperature for the post treatment in this work was 700 °C, which is obviously lower than that in the thermal activation for activated carbon [28–32]. It is commonly believed that the structure of carbon plays a key role for the Reactions (1)–(3). Amorphous carbon and carbon in contact with metal particles are more readily to be oxidized by CO₂. As illustrated in Fig. 7, when CO₂ was introduced into the reactor after CNT growth, it diffused through the channel between CNTs in the array (Fig. 7a) and reacted preferentially with amorphous carbon, forming a concentration gradient along the axial direction of CNT arrays (Fig. 7b).

Due to tubular structure of CNTs, the Reaction (3) was assumed to occur easily at the exterior wall of CNTs, leaving CNTs with good graphitization. Furthermore, due to the formation of CO₂ concentration gradient, the top part of the array was etched more severely. Consequently, the CNTs in the top of the array were composed of fewer graphite walls compared with that in the bottom of arrays. Besides, CO₂ was more readily to attack carbon–catalyst interface because of the catalytic oxidation process. The metal particles have a high density of electrons, and can serve as catalyst for Reaction (1). Thus, the carbon atoms at the root of CNTs are easily oxidized (Fig. 7c) and the chemical bonds between CNT/catalyst/substrate were destroyed, leading to the weakening of array–substrate interaction (Fig. 7d). The free standing CNT arrays with high degree of graphitization can be released easily from substrates by CO₂ oxidation, accordingly.

When O₂ was used as the oxidant, a more complex process for the formation of CO and CO₂ was demonstrated as follows [32]:



where C_f is the free site on the carbon surface where reaction is possible; C(O₂), chemisorbed, localized molecular oxygen; C(O₂)_m, chemisorbed, mobile molecular oxygen; C(O), chemisorbed, localized atom of oxygen and C(O)_m is the chemisorbed, mobile atom of oxygen.

When O₂ is introduced into the reactor, the reaction rates are controlled by transferring rates of oxygen to the carbon surface, as demonstrated in Reactions (4)–(14). The gasification rate of carbon in O₂ atmosphere is much faster compared to CO₂ atmosphere [27,28,32], leading to the rapid oxidation of

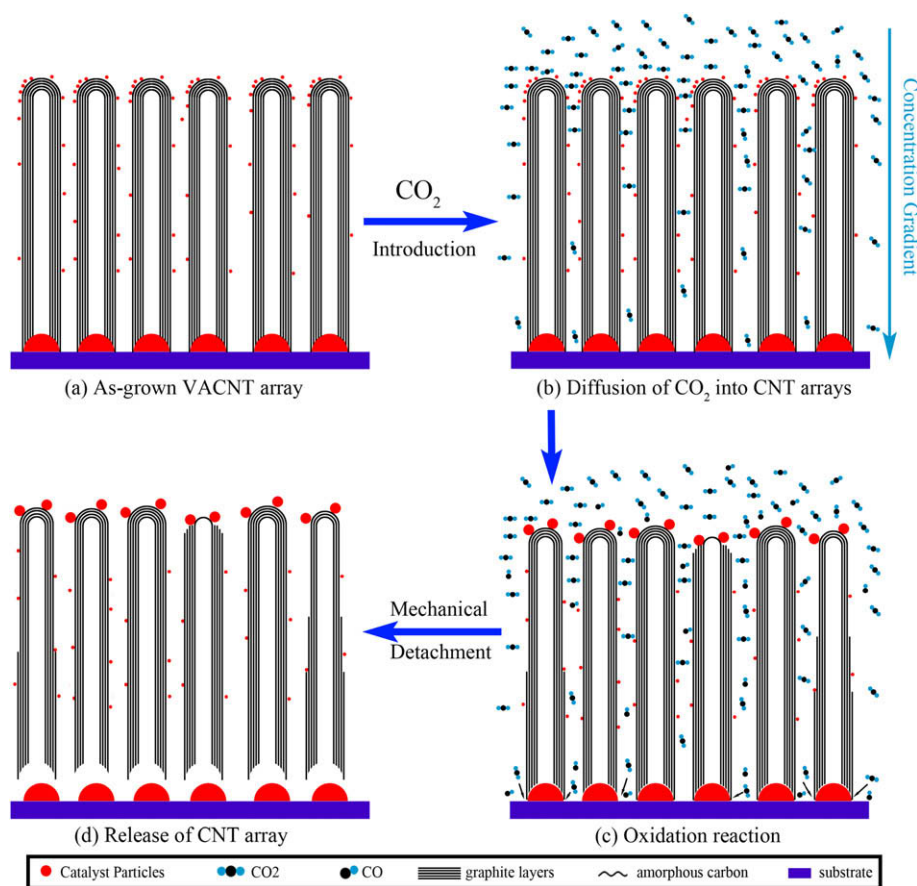


Fig. 7 – The schematic graph of the oxidation process with CO_2 as oxidative reagent.

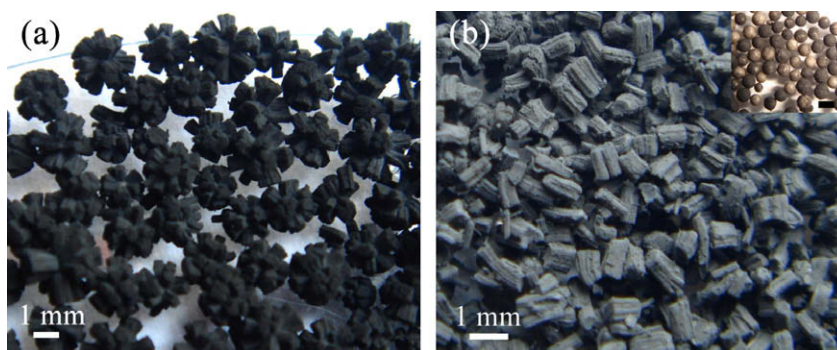


Fig. 8 – (a) The as-grown CNT arrays on ceramic spheres, showing the radial growth behavior; (b) The released CNT arrays by simple mechanical vibration after the CO_2 oxidation. The insert shows the bare ceramic spheres after the detachment of CNT arrays, the scale bar in the insert was 1 mm.

CNT array. The mobile $\text{C}(\text{O}_2)_m$ and $\text{C}(\text{O})_m$ can diffuse along both the radial and axis direction of CNTs, and caused the formation of turbostratic carbon at the exterior layers of CNTs. Thus, CNTs with a turbostratic-graphite heterojunction in array form were obtained. Furthermore, the metal particles at the root were speculated to promote the reduction of mobile $\text{C}(\text{O}_2)_m$ and $\text{C}(\text{O})_m$. This caused the oxidation of carbon at the root of CNT arrays, which led to an easy detachment of free standing CNT arrays.

Finally, it should be noticed that CNT arrays can grow on various substrates, and this presented simple oxidation approach was suitable to release free standing CNT arrays from various substrates. As shown in Fig. 8, free standing CNT arrays can be easily released from spherical ceramic substrates [36] with CO_2 oxidation. During the radial growth on ceramic balls, CNT arrays split into CNT pillars on the spherical substrate. After the oxidation, the connection between CNT pillars and the substrate was weakened and the mechanical

force can be applied to realize the separation. In industry, gas shearing and vibrating screening were anticipated to be suitable for the large-scale applications of such a process. This also indicated that the present oxidation strategy can be easily scaled up to obtain large quantity of free standing CNT arrays on irregular substrates. Furthermore, the degree of oxidation can be easily manipulated by the oxidation temperature and the concentration of oxidant. This release process was promising for the potential applications.

4. Conclusions

CO₂ was used as oxidant to release high quality CNT arrays from the substrate after the growth. Utilizing the difference in the stabilities of different carbon structures, the interaction between array and substrate was dramatically reduced, which facilitated the easy release of CNT arrays. Meanwhile, the selective elimination of amorphous carbon also led to the acquirement of high quality CNT arrays. The value of I_G/I_D in Raman characterization was improved from 1.51 to 2.12. The concentration gradient of CO₂ in the CNT array was taken into consideration to demonstrate the influence of different CO₂ concentration on the oxidation behavior at different parts in the CNT arrays. O₂ oxidation was conducted for comparison; and the reaction showed poor selectivity due to the strong oxidizability. Consequently, severe destruction on the structure of CNTs and the formation of graphitic-turbostatic structure was observed. The different oxidation mechanism of CO₂ and O₂ was also discussed and the result indicated CO₂ to be a more suitable oxidant under this condition. This versatile oxidation process was promising in the large-scale application for the release of free standing CNT arrays from various substrates.

Acknowledgements

The work was supported by the Foundation for the Natural Scientific Foundation of China (Nos. 20736004, 20736007, 2007AA03Z346), the China National Program (No. 2006CB0N0702). The author thanks Prof. P. Thrower for instructive suggestions and Dr. Liemin Au for polishing the whole manuscript.

Appendix A. Supplementary data

Supplementary data associated with this article can be found, in the online version, at [doi:10.1016/j.carbon.2009.12.038](https://doi.org/10.1016/j.carbon.2009.12.038).

REFERENCES

- [1] Qu LT, Dai LM, Osawa E. Shape/size-controlled syntheses of metal nanoparticles for site-selective modification of carbon nanotubes. *J Am Chem Soc* 2006;128(16):5523–32.
- [2] Gong KP, Du F, Xia ZH, Durstock M, Dai LM. Nitrogen-doped carbon nanotube arrays with high electrocatalytic activity for oxygen reduction. *Science* 2009;323(5915):760–4.
- [3] Zhu LB, Sun YY, Hess DW, Wong CP. Well-aligned open-ended carbon nanotube architectures: An approach for device assembly. *Nano Lett* 2006;6(2):243–7.
- [4] Liu K, Jiang KL, Wei Y, Ge SP, Liu P, Fan SS. Controlled termination of the growth of vertically aligned carbon nanotube arrays. *Adv Mater* 2007;19(7):975–8.
- [5] Hata K, Futaba DN, Mizuno K, Namai T, Yumura M, Iijima S. Water-assisted highly efficient synthesis of impurity-free single-walled carbon nanotubes. *Science* 2004;306(5700):1362–4.
- [6] Xiang R, Luo G, Qian W, Wang Y, Wei F, Li Q. Large area growth of aligned CNT arrays on spheres: towards large scale and continuous production. *Chem Vapor Depos* 2007;13(10):533–6.
- [7] Murakami Y, Maruyama S. Detachment of vertically aligned single-walled carbon nanotube films from substrates and their re-attachment to arbitrary surfaces. *Chem Phys Lett* 2006;422(4–6):575–80.
- [8] Zhang Q, Zhou WP, Qian WZ, Xiang R, Huang JQ, Wang DZ, et al. Synchronous growth of vertically aligned carbon nanotubes with pristine stress in the heterogeneous catalysis process. *J Phys Chem C* 2007;111(40):14638–43.
- [9] Wen Q, Qian WZ, Wei F, Liu Y, Ning GQ, Zhang Q. CO₂-assisted SWNT growth on porous catalysts. *Chem Mater* 2007;19(6):1226–30.
- [10] Li ZR, Xu Y, Ma XD, Dervishi E, Saini V, Biris AR, et al. CO₂ enhanced carbon nanotube synthesis from pyrolysis of hydrocarbons. *Chem Commun* 2008(28):3260–2.
- [11] Zhu LB, Xu JW, Xiu YH, Sun YY, Hess DW, Wong CP. Growth and electrical characterization of high-aspect-ratio carbon nanotube arrays. *Carbon* 2006;44(2):253–8.
- [12] Wu J, Ma YF, Tang DM, Liu C, Huang QW, Huang Y, et al. Enhancement of field emission of CNTs array by CO₂-assisted chemical vapor deposition. *J Nanosci Nanotechnol* 2009;9(5):3046–51.
- [13] Huang JQ, Zhang Q, Xu GH, Qian WZ, Wei F. Process intensification by CO₂ for high quality carbon nanotube forest growth: double walled carbon nanotube convexity or single walled carbon nanotube bowl? *Nano Res* 2009;2(11):872–81.
- [14] Lv RT, Kang FY, Wang WX, Wei JQ, Zhang XF, Huang ZH, et al. Soft magnetic performance improvement of Fe-filled carbon nanotubes by water-assisted pyrolysis route. *Phys Status Solidi A* 2007;204(3):867–73.
- [15] Pint CL, Xu YQ, Pasquali M, Hauge RH. Formation of highly dense aligned ribbons and transparent films of single-walled carbon nanotubes directly from carpets. *ACS Nano* 2008;2(9):1871–8.
- [16] Pint CL, Xu YQ, Morosan E, Hauge RH. Alignment dependence of one-dimensional electronic hopping transport observed in films of highly aligned, ultralong single-walled carbon nanotubes. *Appl Phys Lett* 2009;94(18):182107.
- [17] Ren L, Pint CL, Booshenri LG, Rice WD, Wang XF, Hilton DJ, et al. Carbon nanotube terahertz polarizer. *Nano Lett* 2009;9(7):2610–3.
- [18] Tawfik S, O'Brien K, Hart AJ. Flexible high-conductivity carbon-nanotube interconnects made by rolling and printing. *Small* 2009;5(21):2467–73.
- [19] Cao A, Zhang XF, Xu CL, Liang J, Wu DH, Wei BQ. Aligned carbon nanotube growth under oxidative ambient. *J Mater Res* 2001;16(11):3107–10.
- [20] Lv RT, Kang FY, Zhu D, Zhu YQ, Gui XC, Wei JQ, et al. Enhanced field emission of open-ended, thin-walled carbon nanotubes filled with ferromagnetic nanowires. *Carbon* 2009;47(11):2709–15.
- [21] Zhang Q, Xu GH, Huang JQ, Zhou WP, Zhao MQ, Wang Y, et al. Fluffy carbon nanotubes produced by shearing vertically aligned carbon nanotube arrays. *Carbon* 2009;47(2):538–41.

- [22] Hou PX, Liu C, Cheng HM. Purification of carbon nanotubes. *Carbon* 2008;46(15):2003–25.
- [23] Dementev N, Osswald S, Gogotsi Y, Borguet E. Purification of carbon nanotubes by dynamic oxidation in air. *J Mater Chem* 2009;19(42):7904–8.
- [24] Tsang SC, Harris PJF, Green MLH. Thinning and opening of carbon nanotubes by oxidation using carbon-dioxide. *Nature* 1993;362(6420):520–2.
- [25] Walker PL, Shelef M, Anderson RA. Catalysis of carbon gasification. In: Walker PL, editor. *Chem Phys Carbon* 1968;4:287–383.
- [26] Radovic LR, Walker PL, Jenkins RG. Importance of carbon active-sites in the gasification of coal chars. *Fuel* 1983;62(7):849–56.
- [27] Lizzio AA, Piotrowski A, Radovic LR. Effect of oxygen-chemisorption on char gasification reactivity profiles obtained by thermogravimetric analysis. *Fuel* 1988;67(12):1691–5.
- [28] Bessant GAR, Walker PL. Activation of anthracite - using carbon-dioxide versus air. *Carbon* 1994;32(6):1171–6.
- [29] Walker PL. Production of activated carbons: Use of CO₂ versus H₂O as activating agent. *Carbon* 1996;34(10):1297–9.
- [30] Rodriguez-Reinoso F, Pastor AC, Marsh H, Huidobro A. Preparation of activated carbon cloths from viscous rayon Part III Effect of carbonization on CO₂ activation. *Carbon* 2000;38(3):397–406.
- [31] Rodriguez-Valero MA, Martinez-Escandell M, Molina-Sabio M, Rodriguez-Reinoso F. CO₂ activation of olive stones carbonized under pressure. *Carbon* 2001;39(2):320–3.
- [32] Marsh H, Rodriguez-Reinoso F. *Activated Carbon*. Elsevier: Amsterdam; 2006. pp. 243–321.
- [33] Amama PB, Pint CL, McJilton L, Kim SM, Stach EA, Murray PT, et al. Role of water in super growth of single-walled carbon nanotube carpets. *Nano Lett* 2009;9(1):44–9.
- [34] Yasuda S, Hiraoka T, Futaba DN, Yamada T, Yumura M, Hata K. Existence and kinetics of graphitic carbonaceous impurities in carbon nanotube forests to assess the absolute purity. *Nano Lett* 2009;9(2):769–73.
- [35] Futaba DN, Goto J, Yasuda S, Yamada T, Yumura M, Hata K. General rules governing the highly efficient growth of carbon nanotubes. *Adv Mater* 2009;21(47):4811–5.
- [36] Zhang Q, Huang JQ, Zhao MQ, Qian WZ, Wang Y, Wei F. Radial growth of vertically aligned carbon nanotube arrays from ethylene on ceramic spheres. *Carbon* 2008;46(8):1152–8.